

Comparison and evaluation of machine-learning-based spatial downscaling approaches on satellite-derived precipitation data

Honglin Zhu^a, Qiming Zhou^{a,*}, Aihong Cui^a

^a Department of Geography, Hong Kong Baptist University, Hong Kong, China - 20482787@life.hkbu.edu.hk; qiming@hkbu.edu.hk; 17482402@life.hkbu.edu.hk

KEY WORDS: machine learning, PERSIANN-CDR, precipitation, downscaling

ABSTRACT:

Precipitation estimation with high accuracy and resolution is crucial for hydrological and meteorological applications, particularly in ungauged river basins and regions with scarce water resources. Many machine learning (ML) algorithms have been employed in the downscaling of precipitation, however, it remains unclear which algorithm can outperform others. To address this issue, this study evaluates the performance of four ML based downscaling methods to generate high-resolution precipitation estimates at an annual scale. The satellite-derived precipitation data, environmental variables, such as, latitude, longitude, normalized difference vegetation index (NDVI), digital elevation model (DEM), and land surface temperature (LST), as well as the observations from rainfall gauges were used to construct the regression models. The performance of the four ML algorithms including the Support Vector Regression (SVR), Random Forest (RF), Spatial Random Forest (SRF), and Extreme Gradient Boosting (XGBoost) algorithms was compared with three conventional methods: Multiple Linear Regression (MLR), geographically weighted regression (GWR) and Kriging interpolation model. Results showed that ML-based method generally outperformed traditional interpolation methods in precipitation downscaling, as they had higher accuracy and were better at reproducing the spatial distribution of rainfall. Out of ML approaches, XGBoost received the best performance, followed by SRF, RF and SVR, indicating its robustness of capturing nonlinear relationships. After the XGBoost, better performance of SRF than RF and SVR was found. This might be because the SRF just introduced the spatial autocorrelation into the RF models, which illustrated the importance of capturing spatial variations in ML algorithms. These findings regarding the comparison and assessment provided a novel downscaling method for generating high-resolution precipitation data, which could benefit regional flood forecasting, drought monitoring, and irrigation planning.

1. INTRODUCTION

Precipitation is an important component in global water cycle and energy balance (Chen et al., 2021). The amount and distribution of precipitation have significant impact on the water resource management, climate research, and environmental monitoring (Karbalaye Ghorbanpour et al., 2021). Accurate precipitation data is crucial for irrigation planning, reservoir operations, and flood control measures. However, precipitation is also one of the most difficult meteorological factors to detect (Li et al., 2021).

There are some measurements of precipitation data. Rain gauge stations can provide high-quality observations with high temporal resolution, but their spatial coverage is very limited (Sinha et al., 2018). Alternatively, satellite-based precipitation data provide wider spatial coverage. However, satellite-derived precipitation estimates were generated at global scale, and their coarse spatial resolution limits their utility for regional applications such as hydrological modelling and flood forecasting. Thus, the downscaling of satellite precipitation is vital to provide precipitation estimates at finer spatial resolutions.

Generally speaking, there are two distinguished downscaling techniques, the dynamic and statistic downscaling. Both techniques have their own advantages and disadvantages. Dynamic downscaling uses the regional climate model based on strict physical assumptions, and it requires great computing resources and is more computationally expensive (Shashikanth et al., 2014). Statistical downscaling, on the other hand, is achieved by developing statistical relationships between environmental variables (such as temperature, pressure, and moisture) and the precipitation at a lower spatial resolution. These regression relationships are then used to generate

downscaled precipitation data. Statistic downscaling is much easier to use, and has been widely used in many studies (Zhang et al., 2018).

Among statistic downscaling, there has been an increasing popularity in using machine learning techniques to downscale precipitation data. For example, Jing et al. (2016) used Support Vector Machine (SVM) to downscale precipitation based on NDVI, DEM, and Land Surface Temperature (LST) over Tibetan Plateau. Devak et al. (2015) proposed a dynamic framework for downscaling climatic variables by integrating K-Nearest Neighbour and SVM and generating an ensemble of outputs, which performed better than individual models in simulating extreme precipitation events. He et al. (2016) developed an adoptable random forest (RF) model for the downscaling of precipitation, in which the single and double RF models were applied for the mean and extreme precipitation events. Yan et al. (2021) constructed a downscaling-merging scheme based on RF and cokriging to acquire high-resolution precipitation data, and greatly improved its accuracy and spatial details. Chen et al. (2021) introduced the spatial autocorrelation to the RF model and proposed a spatial random forest (SRF) for downscaling. They found that the SRF outperformed other conventional algorithms and illustrated the importance of incorporating spatial autocorrelation to ML approaches. After the Extreme Gradient Boosting (XGBoost) method was proposed, it has been gradually applied in downscaling. The use of XGBoost and Artificial Neural Network (ANN) in the downscaling of Gravity Recovery and Climate Experiment (GRACE) satellite Terrestrial Water Storage (TWSA) estimates for monitoring hydrological droughts was explored, and the XGBoost model was found to outperform the ANN (Ali et al., 2023).

There are many machine learning algorithms used in the downscaling of precipitation data. However, not all ML methods are equally effective, and each method may have its own strengths and weaknesses. Therefore, the objectives of this study were (1) to evaluate and compare five machine learning-based downscaling algorithms in precipitation estimation (2) to investigate the benefits and drawbacks of using machine learning methods to improve the spatial resolution of precipitation data.

2. MATERIALS AND METHODS

2.1 Study area

Guangdong Province is located in the southern part of China, and covers an area of approximately 180,000 km² (Yan et al., 2020). It has a subtropical monsoon climate, characterized by hot and humid summers and mild winters. Guangdong experiences abundant rainfall during the rainy season, which lasts from April to September, and relatively dry weather during the rest of the year (Xin et al., 2021).

The terrain of Guangdong Province is mountainous and hilly, with an average elevation of about 200 m. It has a complex topography, with many valleys, basins, and plains. The precipitation patterns in Guangdong Province is influenced by the monsoon climate and the topography. The rainfall is unevenly distributed both spatially and temporally, with middle areas experiencing heavy rainfall and flooding, and other regions with less rain.

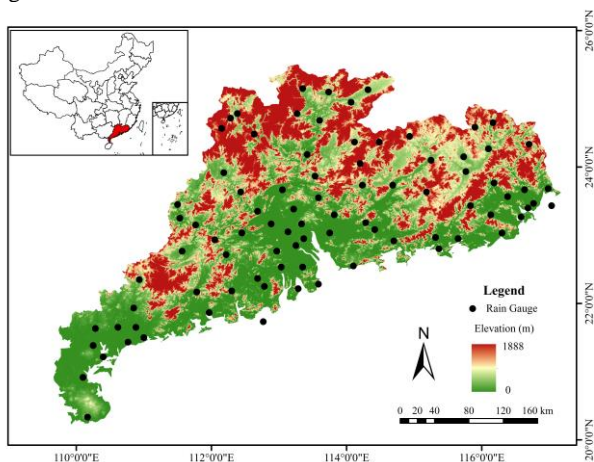


Figure 1. The distribution of rain gauges in Guangdong Province, China

2.2 Dataset and Pre-processing

Table 1. Datasets used in this study

Data	Dataset	Resolution
	Rain Gauges	Daily, Point
Precipitation	PERSIANN-CDR	Daily, 25 km
DEM	SRTM	-, 90 m
NDVI	GIMMS NDVI3g	15d, 8 km
LST	MOD11A2	8d, 1 km

(1) Rain gauge observations

The study region includes 86 rain gauge stations, with a high density in the east and low density in the west, resulting in an uneven distribution (Fig. 1). Daily precipitation data for the period 2006–2010 was collected from the China Meteorological Data Service Centre (CMDSC, 2022), which undergoes strict quality controls (Jiang et al., 2021).

(2) PERSIANN-CDR

PERSIANN-CDR provides a long-term and high-resolution precipitation dataset that spans from 1983 to present with a spatial resolution of 0.25 degrees (Ashouri et al., 2015). PERSIANN-CDR has been validated against a wide range of rain gauge networks and other satellite-based precipitation datasets in different regions and has been shown to have good accuracy and reliability (Miao et al., 2015). In this study, the yearly PERSIANN-CDR data from 2006 to 2010 was obtained from the National Oceanic and Atmospheric Administration (NOAA) National Centres.

(3) Environmental factors

In this study, Normalized Difference Vegetation Index (NDVI), Digital Elevation Model (DEM), and Land Surface Temperature (LST) were commonly used as predictors in downscaling models. They could influence the precipitation through evapotranspiration process, orographic effect, and land surface's energy balance (Duan and Bastiaanssen, 2013; Shah et al., 2019; Zhan et al., 2018). Therefore, incorporating these variables into the downscaling model can improve the accuracy of precipitation estimates.

The Global Inventory Monitoring and Modelling System (GIMMS) NDVI dataset was adopted. It has a spatial resolution of 8 km and a temporal resolution of 15-day (Tucker et al., 2005). The Shuttle Radar Topography Mission (SRTM) based DEM data was applied, with a spatial resolution of 90 m (CGIAR, 2022). The LST data were obtained from the Moderate Resolution Imaging Spectroradiometer (MODIS) at a spatial resolution of 1 km, and a temporal resolution of 8 days (Krishnan et al., 2022).

2.3 Abstract Brief description of downscaling algorithms

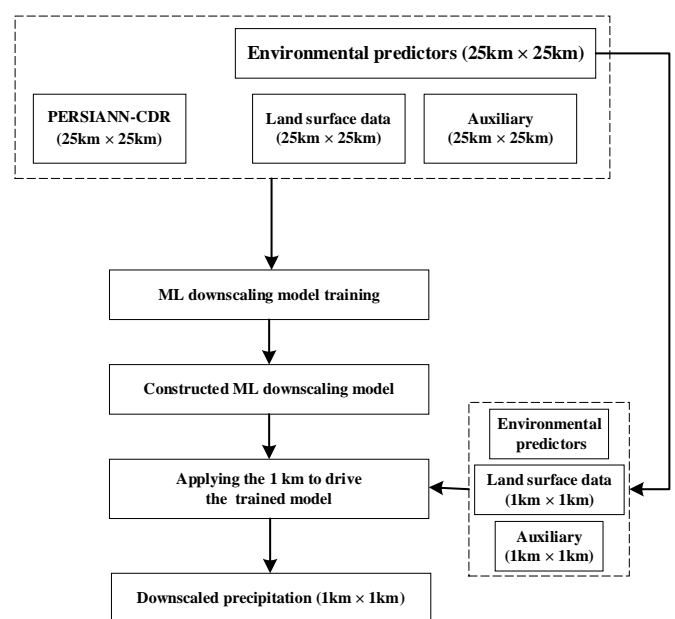


Figure 2. The flowchart of ML based downscaling models.

In this study, we compared four machine learning algorithms for downscaling precipitation: SVM, RF, SRF, and XGBoost. These four models were selected because of their wide applications in precipitation downscaling and their ability to capture nonlinear relationships between predictor and response variables (Cheng et al., 2022; Sachindra et al., 2018). SVM is a popular algorithm for classification and regression tasks, and has been used successfully in precipitation downscaling. RF is an ensemble learning method that can handle a large number of input variables and capture complex interactions between them. SRF is an extension of RF that integrated spatial autocorrelation in modelling. XGBoost is a gradient boosting method that has shown excellent performance in various prediction tasks. By comparing the performance of these four models, we aimed to provide insights into their strengths and weaknesses for precipitation downscaling applications.

2.4 Accuracy measures

In order to assess the accuracy and reliability of the downscaling results, four commonly used indicators were used, including: correlation coefficient (CC), root mean square error (RMSE), mean absolute error (MAE), and Kling-Gupta efficiency (KGE). KGE is a comprehensive evaluation index that considers three components: correlation, variability, and bias (Liu, 2020). Their equations are as followed:

$$CC = \frac{\sum_{i=1}^n (E_i - \bar{E})(O_i - \bar{O})}{\sqrt{\sum_{i=1}^n (E_i - \bar{E})^2} \times \sqrt{\sum_{i=1}^n (O_i - \bar{O})^2}} \quad (1)$$

$$RMSE = \sqrt{\frac{1}{n} \sum_{i=1}^n (E_i - O_i)^2} \quad (2)$$

$$MAE = \frac{\sum_{i=1}^n |E_i - O_i|}{n} \quad (3)$$

$$KGE = 1 - \sqrt{(cc - 1)^2 + \left(\frac{\bar{E}}{\bar{O}} - 1\right)^2 + \left(\frac{CV_E}{CV_O} - 1\right)^2} \quad (4)$$

Where E_i is the estimated precipitation at station i , and O_i is the observed precipitation at station i , n is the number of rain gauge stations.

3. RESULTS AND DISCUSSION

3.1 Accuracy analysis of downscaled results based on different models

Table 2 and Table 3 presented the performance of different models for predicting precipitation from 2006 to 2010. As shown, ML methods generally had better performance than the others, with higher CC and KGE. This might be because ML algorithms were more capable of constructing the complex and nonlinear relationships between environmental predictors and precipitation, whereas traditional methods just assumed linear relationships. Meanwhile, ML models can handle outliers in data and models' overfitting more effectively compared to traditional methods. It is worth noting that the GWR models reported good performance in other studies (Chen et al., 2018; Wang et al., 2022; Xu et al., 2015), but its performance in this study was slightly worse than the ML models. This might be because that ML algorithms included the feature selection techniques that help identify the most important variables for

prediction, but GWR does not have built-in feature selection capabilities. Additionally, ML models had more parameters in model training, such as regularization strength, learning rate to achieve optimal performance. The superior performance of ML downscaling models can help to improve the accuracy and resolution of precipitation data.

Table 2. The performance of different downscaling models using CC and KGE

Dataset		2006	2007	2008	2009	2010
CC	PERSIANN-CDR	0.52	0.47	0.6	0.79	0.51
	Kriging	0.57	0.51	0.56	0.8	0.48
	MLR	0.63	0.55	0.68	0.84	0.53
	GWR	0.66	0.62	0.73	0.89	0.49
	RF	0.78	0.69	0.82	0.91	0.64
	SRF	0.79	0.71	0.84	0.95	0.62
	SVR	0.77	0.65	0.79	0.9	0.68
XGBoost	0.78	0.71	0.8	0.93	0.62	
KGE	PERSIANN-CDR	0.36	0.35	0.57	0.67	0.35
	Kriging	0.38	0.36	0.54	0.7	0.31
	MLR	0.32	0.32	0.57	0.59	0.3
	GWR	0.48	0.45	0.69	0.75	0.31
	RF	0.51	0.46	0.72	0.72	0.35
	SRF	0.56	0.5	0.73	0.79	0.34
	SVR	0.51	0.42	0.71	0.72	0.49
XGBoost	0.57	0.53	0.73	0.79	0.46	

Table 3. The performance of different downscaling models using MAE and RMSE

Dataset		2006	2007	2008	2009	2010
MAE	PERSIA NN-CDR	351.99	247.2	367.76	244.33	357.02
	(mm) Kriging	341.71	240.34	362.81	239.91	355.26
	MLR	313.69	241.83	326.73	267.97	282.81
	GWR	278.62	203.05	281.33	184.33	350.51
	RF	244.63	193.28	222.57	172.37	299.61
	SRF	236.56	186.56	211.41	126.67	353.75
	SVR	245.48	196.61	243.7	184.19	302.78
XGBoost	244.43	188.79	247.21	139.59	270.83	
RMSE	PERSIA NN-CDR	435.96	294.62	446.05	297.34	415.81
	(mm) Kriging	426.48	291.53	444.1	289.8	414.34
	MLR	417.41	291.33	415.81	315.71	332.88
	GWR	355.34	249.63	353.08	223.15	409.47
	RF	308.46	233.58	282.48	205.04	355.91
	SRF	298.42	224.72	268.24	153.89	403.48
	SVR	310.61	245.3	305.09	217.24	353.59
XGBoost	305.13	226.37	309.09	171.29	318.29	

Out of four ML algorithms, XGBoost outperformed other models, showing the highest correlation coefficient (0.78), the highest KGE (0.57), and the lowest MAE and RMSE (244.43 mm and 305.13 mm, respectively). The better performance of XGBoost might be due to the regularization techniques involved in XGBoost, which help to prevent overfitting and improve the generalization performance of the model. The SRF model also showed better performance than SVR and RF, because the spatial autocorrelation has been introduced into the RF model and SRF was better at handling spatially correlated data.

The scatter plot in Figure 3 compared the estimated precipitation from different downscaling models with the observed values. As shown, the result of PERSIANN-CDR was the worst, suggesting that the original satellite data contained large bias and uncertainty. The results presented in the scatter plot are consistent with those in the tables above. ML algorithms had better performance as their scatter plot displayed a more tightly concentrated distribution around the 1:1 line, indicating a closer agreement between the estimated and observed values. Across all the scatter plots of downscaling models, a consistent trend can be found with the original satellite data, in which it tended to underestimate when observed values are larger, and conversely, overestimate when observed values are smaller. This was not surprising because all the downscaling models were constructed based on the satellite precipitation, and the over- and under-estimations would be inherited by the models.

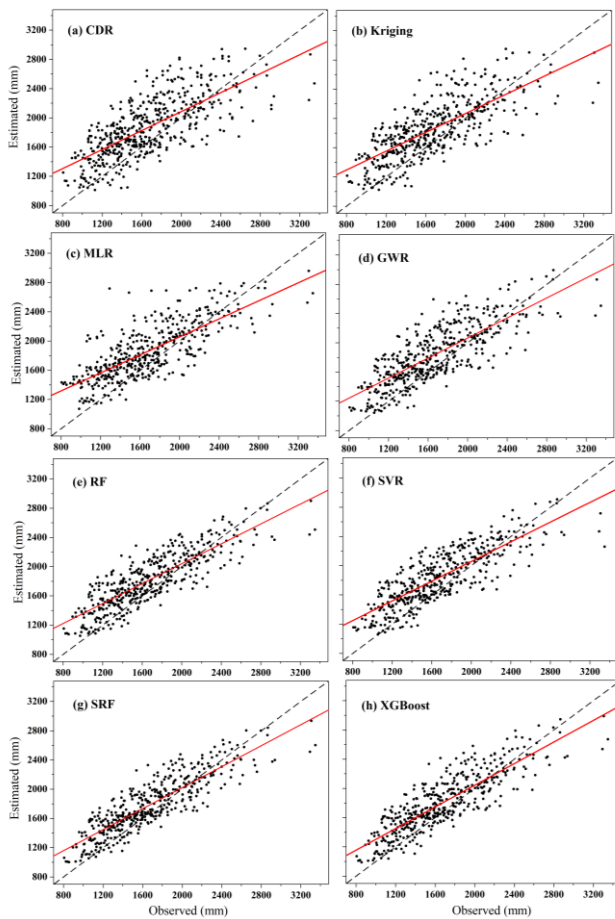


Figure 3. Scatter plots between the observed and estimated precipitation based on different models

3.2 Spatial distribution of downscaled results

In Figure 4, the spatial distribution patterns of the original PERSIANN-CDR and its downscaled results in 2010 were compared. The downscaled precipitation maps shared similar distribution patterns with the original satellite map, with higher precipitation in the middle and lower precipitation in other areas, which was not surprising given that all the regression models were trained from satellite precipitation and would exhibit similar distribution characteristics in the PERSIANN-CDR map. While the original PERSIANN-CDR annual precipitation map contained mosaic-like pixels due to its coarse resolution, the downscaled maps generated by ML-based algorithms provided more spatial information and replicated basic spatial features.

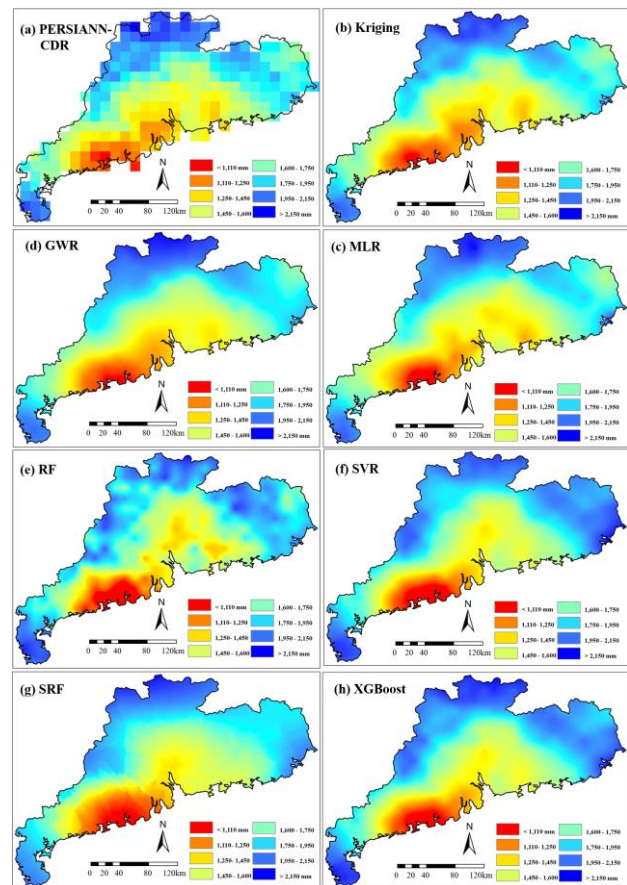


Figure 4. Spatial distribution of downscaled results based on different models.

Particularly, GWR showed good accuracy and successfully captured the spatial features of the PERSIANN-CDR distribution. MLR generally had higher CC and KGE values than Kriging, but it struggled to reproduce the spatial distribution and underestimated precipitation in the middle area. Kriging and the original PERSIANN-CDR both had poor CC and KGE results and produced almost the same spatial pattern, possibly because Kriging interpolation only generated smooth values of the original satellite data. SVR and XGBoost, on the other hand, provided more details with large spatial variations, as seen in the downscaled maps of the regions highlighted by the black circles (Figure 4g-h), where they reproduced low precipitation levels.

3.3 Future work

The results of this study suggest that ML-based approaches have significant potential in improving the accuracy of precipitation downscaling, with XGBoost being the most effective in generating high-resolution precipitation data. However, there are opportunities for further improvement in future studies. Firstly, using a larger and more diverse training dataset would be beneficial to reduce overfitting and improve the generalization of ML models. The size and quality of training data have a significant impact on the performance of machine learning models, and a larger and more diverse dataset can help enhance the accuracy, generalization ability, and robustness of ML models (Liu et al., 2021). Secondly, it is important to involve more observations from rain gauges for testing the ML models. In this study, validation results were based on in-situ data from a limited number of rain gauges, which may not be sufficient to accurately capture the spatial variability of precipitation across the entire region (Sun et al., 2022). This could lead to incomplete and potentially biased results. Furthermore, incorporating multiple satellite-derived precipitation data sources could enhance the accuracy and reliability of downscaling models. Although PERSIANN-CDR was used in this study due to its longer temporal coverage and good consistency with measurements, other remote sensing precipitation products may have their own advantages and limitations (Miao et al., 2015). Combining multiple satellite-derived precipitation data sources could reduce the uncertainty contained in individual products and provide more reliable precipitation estimates (Arshad et al., 2021).

CONCLUSION

This study evaluated the performance of four ML-based downscaling methods, including XGBoost, SRF, RF, and SVR, for generating high-resolution satellite precipitation data. Results showed that ML-based algorithms outperformed conventional methods in terms of CC and KGE, indicating their superior capability in fitting nonlinear relationships between satellite precipitation and environmental variables. Among the four ML-based algorithms, XGBoost and SRF tended to produce the best results having higher CC and KGE and lower MAE and RMSE at most validation years. The downscaled precipitation maps showed comparable distribution patterns with the original PERSIANN-CDR map, reproducing the basic spatial features and more importantly, providing enriched spatial information. It was found that overestimations were obtained at most rain gauges, especially in the middle area and the eastern side. Overall, this study provides valuable insights into the performance of different downscaling methods for satellite precipitation data, which can help improve the accuracy of precipitation estimates in various applications.

REFERENCES

- Ali, S., Khorrami, B., Jehanzaib, M., Tariq, A., Ajmal, M., Arshad, A., Shafeeque, M., Dilawar, A., Basit, I., Zhang, L., Sadri, S., Niaz, M.A., Jamil, A., Khan, S.N., 2023. Spatial Downscaling of GRACE Data Based on XGBoost Model for Improved Understanding of Hydrological Droughts in the Indus Basin Irrigation System (IBIS). *Remote Sens.* 15, 873. <https://doi.org/10.3390/rs15040873>
- Arshad, A., Zhang, W., Zhang, Z., Wang, S., Zhang, B., Cheema, M.J.M., Shalamzari, M.J., 2021. Reconstructing high-resolution gridded precipitation data using an improved downscaling approach over the high altitude mountain regions of Upper Indus Basin (UIB). *Sci. Total Environ.* 784, 147140. <https://doi.org/10.1016/j.scitotenv.2021.147140>
- Ashouri, H., Hsu, K.L., Sorooshian, S., Braithwaite, D.K., Knapp, K.R., Cecil, L.D., Nelson, B.R., Prat, O.P., 2015. PERSIANN-CDR: Daily precipitation climate data record from multisatellite observations for hydrological and climate studies. *Bull. Am. Meteorol. Soc.* 96, 69–83. <https://doi.org/10.1175/BAMS-D-13-00068.1>
- CGIAR, 2022. SRTM Data, CGIAR [Data set] [WWW Document].
- Chen, C., Hu, B., Li, Y., 2021. Easy-to-use spatial Random Forest-based downscaling-calibration method for producing high resolution and accurate precipitation data. *Hydrol. Earth Syst. Sci. Discuss.* 1–50. <https://doi.org/10.5194/hess-2021-332>
- Chen, Y., Huang, J., Sheng, S., Mansaray, L.R., Liu, Z., Wu, H., Wang, X., 2018. A new downscaling-integration framework for high-resolution monthly precipitation estimates: Combining rain gauge observations, satellite-derived precipitation data and geographical ancillary data. *Remote Sens. Environ.* 214, 154–172. <https://doi.org/10.1016/j.rse.2018.05.021>
- Cheng, S., Cheng, L., Qin, S., Zhang, L., Liu, P., Liu, L., Xu, Z., Wang, Q., 2022. Improved Understanding of How Catchment Properties Control Hydrological Partitioning Through Machine Learning. *Water Resour. Res.* 58, 1–21. <https://doi.org/10.1029/2021WR031412>
- CMDSC, 2022. China Meteorological Data Service Center: Gauge data [Data set] [WWW Document].
- Devak, M., Dhanya, C.T., Gosain, A.K., 2015. Dynamic coupling of support vector machine and K-nearest neighbour for downscaling daily rainfall. *J. Hydrol.* 525, 286–301. <https://doi.org/https://doi.org/10.1016/j.jhydrol.2015.03.051>
- Duan, Z., Bastiaanssen, W.G.M., 2013. First results from Version 7 TRMM 3B43 precipitation product in combination with a new downscaling-calibration procedure. *Remote Sens. Environ.* 131, 1–13. <https://doi.org/10.1016/j.rse.2012.12.002>
- He, X., Chaney, N.W., Schleiss, M., Sheffield, J., 2016. Spatial downscaling of precipitation using adaptable random forests. *Water Resour. Res.* 52, 8217–8237.
- Jiang, Y., Yang, K., Shao, C., Zhou, X., Zhao, L., Chen, Y., Wu, H., 2021. A downscaling approach for constructing high-resolution precipitation dataset over the Tibetan Plateau from ERA5 reanalysis. *Atmos. Res.* 256. <https://doi.org/10.1016/j.atmosres.2021.105574>
- Jing, W., Yang, Y., Yue, X., Zhao, X., 2016. A spatial downscaling algorithm for satellite-based precipitation over the Tibetan plateau based on NDVI, DEM, and land surface temperature. *Remote Sens.* 8. <https://doi.org/10.3390/rs8080655>
- Karbalaye Ghorbanpour, A., Hessels, T., Moghim, S., Afshar, A., 2021. Comparison and assessment of spatial downscaling methods for enhancing the accuracy of satellite-based precipitation over Lake Urmia Basin. *J. Hydrol.* 596. <https://doi.org/10.1016/j.jhydrol.2021.126055>
- Krishnan, S., Pradhan, A., Indu, J., 2022. Estimation of high-resolution precipitation using downscaled satellite soil moisture and SM2RAIN approach. *J. Hydrol.* 610, 127926. <https://doi.org/10.1016/j.jhydrol.2022.127926>

- Li, Q., Wang, Z., Shangguan, W., Li, L., Yao, Y., Yu, F., 2021. Improved daily SMAP satellite soil moisture prediction over China using deep learning model with transfer learning. *J. Hydrol.* 600. <https://doi.org/10.1016/j.jhydrol.2021.126698>
- Liu, D., 2020. A rational performance criterion for hydrological model. *J. Hydrol.* 590, 125488. <https://doi.org/10.1016/j.jhydrol.2020.125488>
- Liu, H., Li, Q., Bai, Y., Yang, C., Wang, J., Zhou, Q., Hu, S., Shi, T., Liao, X., Wu, G., 2021. Improving satellite retrieval of oceanic particulate organic carbon concentrations using machine learning methods. *Remote Sens. Environ.* 256, 112316. <https://doi.org/10.1016/j.rse.2021.112316>
- Miao, C., Ashouri, H., Hsu, K.L., Sorooshian, S., Duan, Q., 2015. Evaluation of the PERSIANN-CDR daily rainfall estimates in capturing the behavior of extreme precipitation events over China. *J. Hydrometeorol.* 16, 1387–1396. <https://doi.org/10.1175/JHM-D-14-0174.1>
- Sachindra, D.A., Ahmed, K., Rashid, M.M., Shahid, S., Perera, B.J.C., 2018. Statistical downscaling of precipitation using machine learning techniques. *Atmos. Res.* 212, 240–258. <https://doi.org/10.1016/j.atmosres.2018.05.022>
- Shah, H.L., Zhou, T., Huang, M., Mishra, V., 2019. Strong Influence of Irrigation on Water Budget and Land Surface Temperature in Indian Subcontinental River Basins. *J. Geophys. Res. Atmos.* 124, 1449–1462. <https://doi.org/10.1029/2018JD029132>
- Shashikanth, K., Madhusoodhanan, C.G., Ghosh, S., Eldho, T.I., Rajendran, K., Murtugudde, R., 2014. Comparing statistically downscaled simulations of Indian monsoon at different spatial resolutions. *J. Hydrol.* 519, 3163–3177. <https://doi.org/10.1016/j.jhydrol.2014.10.042>
- Sinha, P., Mann, M.E., Fuentes, J.D., Mejia, A., Ning, L., Sun, W., He, T., Obeysekera, J., 2018. Downscaled rainfall projections in south Florida using self-organizing maps. *Sci. Total Environ.* 635, 1110–1123. <https://doi.org/10.1016/j.scitotenv.2018.04.144>
- Sun, B., Zhang, Y., Zhou, Q., Zhang, X., 2022. Effectiveness of Semi-Supervised Learning and Multi-Source Data in Detailed Urban Landuse Mapping with a Few Labeled Samples. *Remote Sens.* 14. <https://doi.org/10.3390/rs14030648>
- Tucker, C.J., Pinzon, J.E., Brown, M.E., Slayback, D.A., Pak, E.W., Mahoney, R., Vermote, E.F., ElSaleous, N., 2005. An extended AVHRR 8-km NDVI dataset compatible with MODIS and SPOT vegetation NDVI data. *Int. J. Remote Sens.* 26, 4485–4498. <https://doi.org/10.1080/01431160500168686>
- Wang, H., Zang, F., Zhao, C., Liu, C., 2022. A GWR downscaling method to reconstruct high-resolution precipitation dataset based on GSMaP-Gauge data: A case study in the Qilian Mountains, Northwest China. *Sci. Total Environ.* 810, 152066. <https://doi.org/10.1016/j.scitotenv.2021.152066>
- Xin, Y., Lu, N., Jiang, H., Liu, Y., Yao, L., 2021. Performance of ERA5 reanalysis precipitation products in the Guangdong-Hong Kong-Macao greater Bay Area, China. *J. Hydrol.* 602, 126791. <https://doi.org/10.1016/j.jhydrol.2021.126791>
- Xu, S., Wu, C., Wang, L., Gonsamo, A., Shen, Y., Niu, Z., 2015. A new satellite-based monthly precipitation downscaling algorithm with non-stationary relationship between precipitation and land surface characteristics. *Remote Sens. Environ.* 162, 119–140. <https://doi.org/10.1016/j.rse.2015.02.024>
- Yan, M., Chan, J.C.L., Zhao, K., 2020. Impacts of Urbanization on the Precipitation Characteristics in Guangdong Province, China. *Adv. Atmos. Sci.* 37, 696–706. <https://doi.org/10.1007/s00376-020-9218-3>
- Yan, X., Chen, H., Tian, B., Sheng, S., Wang, J., Kim, J.S., 2021. A downscaling–merging scheme for improving daily spatial precipitation estimates based on random forest and cokriging. *Remote Sens.* 13. <https://doi.org/10.3390/rs13112040>
- Zhan, C., Han, J., Hu, S., Liu, L., Dong, Y., 2018. Spatial Downscaling of GPM Annual and Monthly Precipitation Using Regression-Based Algorithms in a Mountainous Area. *Adv. Meteorol.* 2018. <https://doi.org/10.1155/2018/1506017>
- Zhang, T., Li, B., Yuan, Y., Gao, X., Sun, Q., Xu, L., Jiang, Y., 2018. Spatial downscaling of TRMM precipitation data considering the impacts of macro-geographical factors and local elevation in the Three-River Headwaters Region. *Remote Sens. Environ.* 215, 109–127. <https://doi.org/10.1016/j.rse.2018.06.004>